

AperTO - Archivio Istituzionale Open Access dell'Università di Torino

Anti-zika virus activity of polyoxometalates

This is the author's manuscript

Original Citation:

Availability:

This version is available <http://hdl.handle.net/2318/1701118> since 2022-01-26T11:13:42Z

Published version:

DOI:10.1016/j.antiviral.2019.01.005

Terms of use:

Open Access

Anyone can freely access the full text of works made available as "Open Access". Works made available under a Creative Commons license can be used according to the terms and conditions of said license. Use of all other works requires consent of the right holder (author or publisher) if not exempted from copyright protection by the applicable law.

(Article begins on next page)

This is the author's final version of the contribution published as:

Rachele Francese, Andrea Civra, Massimo Rittà, Manuela Donalisio, Monica Argenziano, Roberta Cavalli, Ali S. Mougharbel, Ulrich Kortz, David Lembo. Anti-zika virus activity of polyoxometalates. *Antiviral Res.* 2019 Mar;163:29-33. doi: 10.1016/j.antiviral.2019.01.005.

The publisher's version is available at:

<https://www.sciencedirect.com/science/article/pii/S0166354218306776>

When citing, please refer to the published version.

Link to this full text:

<http://hdl.handle.net/>

This full text was downloaded from iris-AperTO: <https://iris.unito.it/>

1 **Anti-zika virus activity of polyoxometalates**

2 Rachele Francese ^a, Andrea Civra ^a, Massimo Rittà ^a, Manuela Donalisio ^a, Monica Argenziano ^b,
3 Roberta Cavalli ^b, Ali S. Mougharbel ^c, Ulrich Kortz ^{c*}, David Lembo ^{a*}

4 ^a*Dept. of Clinical and Biological Sciences; Laboratory of Molecular Virology and Antiviral Research;*
5 *University of Turin; S. Luigi Gonzaga Hospital; Orbassano (Turin), Italy.*

6 ^b*Dept. of Drug Science and Technology; Innovative Pharmaceutical and Cosmetic Technology and*
7 *Nanotechnology Group; University of Turin, Italy.*

8 ^c*Department of Life Sciences and Chemistry, Jacobs University, Campus Ring 1, 28759 Bremen,*
9 *Germany.*

10 **Corresponding authors*

11 David Lembo, Email: david.lembo@unito.it

12 Ulrich Kortz, Email: u.kortz@jacobs-university.de

13

14 **Keywords:** zika virus, antivirals, polyoxometalates, entry inhibitor, flavivirus

15 **Abstract**

16 **Zika virus (ZIKV) is an emerging infectious viral pathogen associated with severe fetal cerebral**
17 **anomalies and the paralytic Guillain-Barré syndrome in adults. It was the cause of a recent**
18 **global health crisis following its entrance into a naïve population in the Americas. Nowadays, no**
19 **vaccine or specific antiviral against ZIKV is available. In this study, we identified three**
20 **polyoxometales (POMs), the Anderson-Evans type $[\text{TeW}_6\text{O}_{24}]^{6-}$ (TeW_6), and the Keggin-type**
21 **$[\text{TiW}_{11}\text{CoO}_{40}]^{8-}$ (TiW_{11}Co), and $[\text{Ti}_2\text{PW}_{10}\text{O}_{40}]^{7-}$ ($\text{Ti}_2\text{PW}_{10}$), that inhibit ZIKV infection with EC_{50}s in**
22 **the low micromolar range. $\text{Ti}_2\text{PW}_{10}$, the POM with the greater selectivity index (SI), was selected**
23 **and the step of ZIKV replicative cycle putatively inhibited was investigated by specific antiviral**
24 **assays. We demonstrated that $\text{Ti}_2\text{PW}_{10}$ targets the entry process of ZIKV infection and it is able**
25 **to significantly reduce ZIKV progeny production. These results suggest that the polyanion**
26 **$\text{Ti}_2\text{PW}_{10}$ could be a good starting point to develop an effective therapeutic to treat ZIKV**
27 **infection.**

28

29 ZIKV is an enveloped positive-strand RNA virus belonging to the *Flaviviridae* family and
30 mostly transmitted by *Aedes aegypti* mosquitoes.¹ Sexual, vertical and blood transmissions
31 have also been reported.²⁻⁴ In symptomatic individuals (around 18% of cases), ZIKV causes
32 a mild illness characterized by fever, rash, headache, conjunctivitis, joint and muscle pain;⁵
33 this clinical presentation is similar to that of other arbovirus infections, such as
34 chikungunya and dengue virus. However, unlike other flavivirus, ZIKV is associated to two
35 main neurological complications: the Guillain-Barré Syndrome in adults and the now
36 termed Zika Congenital Syndrome (CSZ), a variety of neurological impairments in fetus and
37 infants of women infected during pregnancy. The main congenital manifestations,
38 developed in nearly one third of these newborns, are severe microcephaly, resulting in a
39 partially collapsed skull, intracranial calcifications, eyes abnormalities, redundant scalp
40 skin, arthrogryposis and clubfoot.^{3,6,7,8} Specifically, the risk of microcephaly, with a
41 catastrophic impact on the socioeconomic status of affected families, was reported to be
42 1–13% during the first trimester and negligible during second and third trimesters.⁹
43 ZIKV can be classified into two lineages (African and Asian) and three genotypes (West
44 African, East African, and Asian), differing in pathogenicity and virulence. The Asian-lineage
45 ZIKV, responsible for the latest epidemics (on Yap Island and Micronesia in 2007, in French
46 Polynesia in 2013 and in the Americas in 2016), is considered to be less virulent than the
47 African one, because of the lower infection rate, the lower viral production, the poor
48 induction of early cell death and the lower immuno-stimulation in different models. These
49 characteristics allow the virus to cause a prolonged infection within the central nervous
50 system of fetus that could be the cause of its association with neurological impairments.
51 On the contrary, the African lineage-ZIKV can result in a more acute infection.¹⁰⁻¹⁴
52 The last major epidemic in the Americas, in 2016, counted 177614 confirmed ZIKV cases
53 and 2552 cases of CSZ at the end of the year, driving the World Health Organization to
54 declare a public health emergency of international concern.^{15,16} Since then, great efforts
55 have been carried out, but nowadays still no vaccine or specific antiviral against ZIKV is
56 available.^{17,18} The best way to prevent ZIKV infection is to avoid mosquito bites and the
57 treatment of infected patients is palliative, involving analgesics and antipyretics. In this
58 context, ZIKV infection presents a huge challenge to the global health system and the
59 search for efficient antivirals is absolutely necessary. To this aim, we investigated *in vitro*
60 the anti-ZIKV activity of a minilibrary of three polyoxometalates (POMs). POMs are

61 discrete, anionic metal-oxo complexes of early *d* block metal ions in high oxidation states
62 (e.g. W^{VI} , Mo^{VI} , V^V) with a very large structural and compositional variety and a multitude
63 of associated physicochemical properties.¹⁹⁻²¹ POMs are usually synthesized in aqueous
64 acidic media, but some selected species are also stable at pH 7-8. In fact, POMs have been
65 investigated for many years as potentially useful agents in medicine, mainly for their
66 antiviral, antitumoral, and antibacterial properties.²²⁻²⁸ Here, we decided to investigate the
67 following three solution-stable POMs, the Anderson-Evans type $[TeW_6O_{24}]^{6-}$ (TeW_6),²⁹ and
68 the Keggin-type $[TiW_{11}CoO_{40}]^{8-}$ ($TiW_{11}Co$),³⁰ and $[Ti_2PW_{10}O_{40}]^{7-}$ (Ti_2PW_{10}),³¹ which were all
69 synthesized according to the published procedures. The size of all three polyanions is in the
70 range of 1 nm diameter. The purity ($\geq 95\%$) of the compounds was confirmed by NMR and
71 IR (Data available in Supplementary info). Some of these POMs have already been used in
72 biological studies. For instance, **Ti₂PW₁₀** showed interesting results in the inhibition of
73 acetylcholinesterase activity while maintaining low toxicity levels.³² On the other hand,
74 **TeW₆** showed good activity against diabetes and Alzheimer's disease.^{33, 34}

75 In order to perform in vitro biological assays, we first prepared aqueous solutions of **TeW₆**,
76 **TiW₁₁Co**, and **Ti₂PW₁₀** and we determined their physico-chemical characteristics (pH,
77 osmolarity, Zeta potential) (Table1) and their biocompatibility. The POMs were stable in
78 aqueous solution up to 6 months stored at 4°C. Indeed, a concentration decrease of 3.25,
79 5.05 and 4.45 % was observed for **TeW₆**, **TiW₁₁Co** and **Ti₂PW₁₀** respectively, after 6 months.

80 In the hemolysis assay, no significant hemolysis caused by the POM solutions was
81 observed, indicating good biocompatibility. (Data available in Supplementary info). The
82 tonicity and pH values were suitable for the following cell experiments.

83 Therefore, to evaluate the anti-Zika virus activity of the three POMs, we performed virus
84 inhibition assays against two Zika virus strains, the 1947 Uganda MR766 and the 2013
85 French Polynesia HPF2013, representing the African and the Asian lineage respectively. The
86 cells were treated with decreasing concentrations of POMs before, during and after
87 infection, in order to use a complete protection assay. As shown in Table 2, all three POMs
88 were active against both ZIKV strains with half maximal effective concentrations (EC_{50} s)
89 ranging from 0.63 to 2.52 μ M. Moreover, in order to assess the specificity of the anti-ZIKV
90 activity of the POMs, they were tested against the human rotavirus (HRoV), an unrelated
91 RNA virus belonging to the Reoviridae family. Interestingly, we did not observe any
92 inhibition. Next, to exclude the possibility that this antiviral activity was due to a cytotoxic

93 effect of the POMs, viability assays were carried out on uninfected cells, challenged with
94 the compounds under the same conditions as the virus inhibition assays. The CC_{50} s were
95 different for all three POMs (**TeW₆** CC_{50} = 210.1 μ M, **TiW₁₁Co** CC_{50} = 97.08 μ M, **Ti₂PW₁₀** CC_{50}
96 >225 μ M), and demonstrated that they are not toxic at the concentrations used in the
97 antiviral assays. The Selectivity Index (SI) of **Ti₂PW₁₀** was the most favorable one, so we
98 decided to concentrate our research on the study of the mechanism of action of this
99 polyanion. All the experiments were performed with the two Zika virus strains used for the
100 initial screening. We first investigated whether the antiviral activity of **Ti₂PW₁₀** was exerted
101 via direct inactivation of the viral particles. The ZIKV particles were incubated with a
102 concentration of **Ti₂PW₁₀** that reduces almost completely the virus infection (EC_{90}) and
103 then the viral titer was determined at high dilutions at which the polyanion was no longer
104 active when added to cells. As depicted in Figure 1A, there was no significant difference
105 between the titer of treated virus and the titer of untreated control, demonstrating that
106 **Ti₂PW₁₀** is not able to impair extracellular viral particles. Having excluded the viral particle
107 as the target of the antiviral activity of **Ti₂PW₁₀**, further experiments were performed to
108 investigate whether this polyanion acted directly on cells or on essential steps of the ZIKV
109 replicative cycle. Vero cells were pre-treated with decreasing dilutions of the polyanion for
110 2 hours before virus infection; as reported in Figure 1B, the infection of both ZIKV strains
111 was not inhibited even at the highest tested concentration. Hence, we explored the
112 possibility that **Ti₂PW₁₀** treatment could affect the early steps of the ZIKV replicative cycle.
113 Binding assays were performed allowing the virus to bind host cell surface in the presence
114 of a high concentration of **Ti₂PW₁₀**. The results (Figure 2A) demonstrated that the
115 treatment did not significantly reduce ($p > 0.05$) the titer of viral particles bound to the cell
116 surface, thus suggesting that inhibition occurs at a post-binding stage. To verify this
117 hypothesis, we treated cells immediately after virus attachment, i.e. during virus entry into
118 the host cell. In this case (Figure 2B), we observed a marked antiviral activity of **Ti₂PW₁₀**
119 against both, MR766 and HPF2013, ZIKV strains (EC_{50} = 1.11 and 1.25 μ M respectively). To
120 exclude an additional antiviral action of **Ti₂PW₁₀** on the last steps of the ZIKV replicative
121 cycle, we executed focus reduction assays adding the polyanion to cells immediately after
122 virus entry into the host cell (post-entry assay). We stopped the treatment at 24 hours
123 post-infection, i.e. at the end of the first replicative cycle, in order to avoid inhibition of the
124 entry step of the upcoming viral progeny. As shown in Figure 2C, the post-entry treatment

125 did not reduce virus infectivity, suggesting that only the entry step is targeted by **Ti₂PW₁₀**.
126 To confirm the inhibition of the ZIKV entry step, immunofluorescence experiments were
127 performed by adding the polyanion (EC₉₉) during the virus entry step or immediately after
128 the entry phase (post-entry). As reported in Figure 2D (MR766 experiments) and Figure 2E
129 (experiments with HPF2013), it was possible to detect a strong red signal of ZIKV protein E
130 only in the untreated and in the post-entry treated samples. The number of red infected
131 cells in the post-entry treated samples was comparable to the one of the untreated
132 control. On the contrary, the number of infected cells in the entry-treated samples was
133 considerably reduced. All together these data indicate that the entry step is the target of
134 the **Ti₂PW₁₀** antiviral activity. Finally, to complete the *in vitro* analysis of the antiviral
135 potential of **Ti₂PW₁₀** against ZIKV strains, virus yield reduction assays were performed by
136 treating cells during and after infection and allowing multiple cycles of viral replication to
137 occur before measuring the production of infectious viruses. The results (Figure 3)
138 demonstrated that **Ti₂PW₁₀** significantly reduces the viral progeny production of both ZIKV
139 strains ($p < 0.001$).

140 Previously, researchers focused on the antiviral properties of POMs because they are
141 generally nontoxic to normal cells. Indeed, several studies reported the broad spectrum
142 antiviral activities of POMs against different types of respiratory-viruses, as RSV, FluV A,
143 FluV B, PfluV and SARS,^{35,36} against HCV and DENV,³⁶⁻³⁸ belonging to the same family of
144 ZIKV, and against others, as HIV, HSV-1, HSV-2 and HBV.^{23,38,39} Herein, we showed that
145 three heteropolytungstates, never tested before as antiviral agents, are endowed with a
146 strong antiviral activity against ZIKV and we demonstrated their good biocompatibility. For
147 the first time, POMs have been tested against two ZIKV strains and we can now include
148 ZIKV in the list of pathogens targeted by the wide spectrum of action of POMs. Of note, we
149 did not observe any inhibition against the human rotavirus, a taxonomically unrelated RNA
150 virus. All together these results indicate that **TeW₆**, **TiW₁₁Co** and **Ti₂PW₁₀** exert a specific
151 and not strain-restricted anti-ZIKV effect. In future experiments, we will investigate the
152 antiviral action of **TeW₆**, **TiW₁₁Co** and **Ti₂PW₁₀** against other RNA and DNA viruses.

153 Some other POMs have already been investigated for their mechanism of action, which
154 commonly depends on their shape, size and composition. Various studies reported on the
155 inhibition of the early steps of an infection: for instance, *Shigeta et al.*,³⁸ demonstrated that
156 the tri-vanadium-containing sandwich-type polyanion $[(VO)_3(SbW_9O_{33})_2]^{11-}$ affects the

157 binding of HIV to the cell membrane and the syncytium formation between HIV-infected
158 and uninfected cells; another biochemical study,³⁹ reports that the ability of the tri-
159 niobium-containing Keggin ion $[\text{SiW}_9\text{Nb}_3\text{O}_{40}]^{7-}$ to prevent the binding and fusion process of
160 different viruses is mainly due to its localization on the cell surface; finally, *Barnard et al.*,³⁵
161 indicate the alteration of the attachment step as the primary mode of RSV inhibition by
162 POMs of several structural classes. Consistent with these findings, we demonstrated that
163 **Ti₂PW₁₀** acts as inhibitor of the entry process of ZIKV into the host cell. By contrast, no
164 inhibition was observed at the binding stage. Further experiments are necessary to identify
165 the cellular localization of this polyanion and to clarify its molecular mechanism of action.
166 In conclusion, we have discovered that the Keggin-type POM **Ti₂PW₁₀** inhibits ZIKV infection
167 by hampering the entry process of the virus into the host cell. Since specific antivirals
168 against ZIKV are not available, this polyanion could be a good starting point for the
169 development of novel and efficient antiviral pharmaceuticals.

170

171

172

173

174

175

176

177 **Abbreviations**

178 ZIKV, zika virus; HRoV, human rotavirus; RSV, respiratory syncytial virus, FluV A; influenza virus
179 type A, FluV B; influenza virus type B; PfluV, parainfluenza virus; SARS, severe acute respiratory
180 syndrome; HCV, hepatitis C virus; DENV, dengue virus; HIV, human immunodeficiency virus; HSV-1,
181 herpes simplex virus type 1; HSV-2, herpes simplex virus type 2; HBV, hepatitis B virus; POMs,
182 polyoxometalates; EC₅₀, half maximal effective concentration; EC₉₀, 90 % effective concentration;
183 CC₅₀, half maximal cytotoxic concentration; SI, selectivity index; n.a., not assessable; CI, confidence
184 interval; PFU, plaque forming unit; PFU/ml, plaque forming unit per ml;

185 **Declaration of interest**

186 None.

187 **Acknowledgements**

188 This work was financially supported by the University of Turin. [Grant number RILO 2018]

189 **Appendix A. Supplementary data:** Supplementary data related to this article can be found at

190 **References**

- 191 1 J-C. Saiz, Á. Vázquez-Calvo, A.B. Blázquez, T. Merino-Ramos, E. Escribano-Romero, M.
192 A. Martín-Acebes, *Front Microbiol*, Zika Virus: the Latest Newcomer, 2016, **7**, 496. doi:
193 10.3389/fmicb.2016.00496
- 194 2 D. Musso, C. Roche, E. Robin, T. Nhan, A. Teissier, V-M. Cao-Lormeau, *Emerg Infect Dis*,
195 Potential Sexual Transmission of Zika Virus, 2015, **21**, 359–61. doi: 10.3201/eid2102.141363
- 196 3 J. Mlakar, M. Korva, N. Tul, M. Popović, M. Poljšak-Prijatelj, J. Mraz, M. Kolencet, K. R. Rus,
197 T. V. Vipotnik, V. F. Vodusek, A. Vizjak, J. Pižem, M. Petrovec, T. A. Županc, *N Engl J Med*,
198 Zika Virus Associated with Microcephaly, 2016, **374**, 951–8. doi: 10.1056/NEJMoa1600651
- 199 4 I. J. F. Motta, B. R. Spencer, S. G. Cordeiro da Silva, M. B. Arruda, J. A. Dobbin, Y. B. M.
200 Gonzaga, I. P. Arcuri, R. C. B. S. Tavares, E. H. Atta, R. F. M. Fernandes, D. A. Costa, L. J.
201 Ribeiro, F. Limonte, L. M. Higa, C. M. Voloch, R. M. Brindeiro, A. Tanuri, O. C. Ferreira, *N Engl J*
202 *Med*, Evidence for Transmission of Zika Virus by Platelet Transfusion, 2016, **375**, 1101–3. doi:
203 10.1056/NEJMc1607262
- 204 5 E. S. Paixão, F. Barreto, M. da Glória Teixeira, N. da Conceição, M. Costa, L. C.
205 Rodrigues, *Am J Public Health*, Epidemiology, and Clinical Manifestations of Zika: A Systematic
206 Review, 2016, **106**, 606–12. doi: 10.2105/AJPH.2016.303112
- 207 6 S. A. Rasmussen, D. J. Jamieson, M. A. Honein, L. R. Petersen.. *N Engl J Med*, Zika Virus
208 and Birth Defects — Reviewing the Evidence for Causality, 2016, **374**, 1981–7. doi:
209 10.1056/NEJMSr1604338
- 210 7 V. M. Cao-Lormeau, A. Blake, S. Mons, S. Lastere, C. Roche, J. Vanhomwegen, T. Dub, L.
211 Baudouin, A. Teissier, P. Larre, A.L. Vial, C. Decam, V. Choumet, S.K. Halstead, H. J. Willison, L.
212 Musset, J. C. Manuguerra, P. Despres, E. Fournier, H. P. Mallet, D. Musso, A. Fontanet, J. Neil,
213 F. Ghawché, *Lancet Lond Engl*, Guillain-Barré Syndrome outbreak caused by ZIKA virus
214 infection in French Polynesia, 2016, **387**, 1531–9. doi: 10.1016/S0140-6736(16)00562-6
- 215 8 P. Brasil , J. P. Pereira, M. E. Moreira, R. M. R. Nogueira, L. Damasceno, M. Wakimoto,
216 R. S. Rabello, S. G. Valderramos, U.-A. Halai, T. S. Salles, A. A. Zin, D. Horovitz, P. Daltro, M.
217 Boechat, C. Raja Gabaglia, P. Carvalho de Sequeira, J. H. Pilotto, R. Medialdea-Carrera, D.
218 Cotrim da Cunha, L. M. Abreu de Carvalho, M. Pone, A. Machado Siqueira, G. A. Calvet, A. E.
219 Rodrigues Baião, E. S. Neves, P. R. Nassar de Carvalho, R. H. Hasue, P. B. Marschik, C.
220 Einspieler, C. Janzen, J. D. Cherry, A. M. Bispo de Filippis, K. Nielsen-Saines, *N Engl J Med*, Zika

221 Virus Infection in Pregnant Women in Rio de Janeiro, 2016, **375**, 2321–34. doi:
222 10.1056/NEJMoa1602412

223 9 M. McCarthy, *BMJ*, Microcephaly risk with Zika infection is 1-13% in first trimester,
224 study shows, 2016, *353*, i3048. doi: <https://doi.org/10.1136/bmj.i3048>

225 10 M. R. Duffy, T. -H. Chen, W. T. Hancock, A. M. Powers, J. L. Kool, R. S. Lanciotti, M.
226 Pretrick, M. Marfel, S. Holzbauer, C. Dubray, L. Guillaumot, A. Griggs, M. Bel, A. J. Lambert, J.
227 Laven, O. Kosoy, A. Panella, B. J. Biggerstaff, M. Fischer, E. B. Hayes, *N Engl J Med*, Zika virus
228 outbreak on Yap Island, Federated States of Micronesia, 2009, **360**, 2536–43. doi:
229 10.1056/NEJMoa0805715

230 11 V. M. Cao-Lormeau, C. Roche, A. Teissier, E. Robin, A. L. Berry, H. P. Mallet, A. A. Sall, D.
231 Musso, *Emerg Infect Dis*, Zika virus, French polynesia, South pacific, 2013, 2014, **20**, 1085–6.
232 doi: 10.3201/eid2006.140138.

233 12 Y. Simonin, D. van Riel, P. Van de Perre, B. Rockx, S. Salinas, *PLoS Negl Trop Dis*,
234 Differential virulence between Asian and African lineages of Zika virus 2017, **11**. doi:
235 10.1371/journal.pntd.0005821

236 13 Q. Shao, S. Herrlinger, Y.N. Zhu, M. Yang, F. Goodfellow, S. L. Stice, X.P. Qi, M. A. Brindley,
237 J.F. Chen, *The Company of Biologists*, 2017, **144**, 4114-4124, The African Zika virus MR-766
238 is more virulent and causes more severe brain damage than current Asian lineage and
239 dengue virus. doi:10.1242/dev.156752

240 14 J. T. Beaver, N. Lelutiu, R. Habib, I. Skountzou, *Front. Immunol.*, Evolution of Two Major
241 Zika Virus Lineages: Implications for Pathology, Immune Response, and Vaccine
242 Development, 2018, **9**, 1640. doi: 10.3389/fimmu.2018.01640

243 15 CDC, <https://www.cdc.gov/zika/reporting/case-counts.html>, (accessed May 2018).

244 16 PAHO WHO,
245 [https://www.paho.org/hq/index.php?option=com_content&view=article&id=12390%3Azika-](https://www.paho.org/hq/index.php?option=com_content&view=article&id=12390%3Azika-cumulative-cases&catid=8424%3Acontents&Itemid=42090&lang=en)
246 [cumulative-cases&catid=8424%3Acontents&Itemid=42090&lang=en](https://www.paho.org/hq/index.php?option=com_content&view=article&id=12390%3Azika-cumulative-cases&catid=8424%3Acontents&Itemid=42090&lang=en), (accessed May 2018)

247 17 J. M. Richner, M. S. Diamond, *Curr Opin Immunol*, Zika virus vaccines: immune
248 response, current status, and future challenges, 2018, **53**, 130–6. doi:
249 10.1016/j.coi.2018.04.024

250 18 J. C. Saiz, M. A. Martín-Acebes, *Antimicrob Agents Chemother*, The Race To Find
251 Antivirals for Zika Virus, 2017, **61**. doi: 10.1128/AAC.00411-17

252 19 M. T. Pope, *Heteropoly and Isopoly Oxometalates*, Springer, Berlin, 1983.

253 20 M. T. Pope, A. Müller, *Angew. Chem. Int. Ed. Engl*, Polyoxometalate Chemistry: An Old
254 Field with New Dimensions in Several Disciplines, 1991, **30**, 34–48.
255 <https://doi.org/10.1002/anie.199100341>

256 21 M. T. Pope, U. Kortz, *Polyoxometalates, in Encyclopedia of Inorganic and Bioinorganic*
257 *Chemistry*, John Wiley, 2012. <https://doi.org/10.1002/9781119951438.eibc0185.pub2>

258 22 S. G. Sarafianos, U. Kortz, M. T. Pope, M. J. Modak, *Biochem. J.*, Mechanism of
259 polyoxometalate-mediated inactivation of DNA polymerases: an analysis with HIV-1 reverse
260 transcriptase indicates specificity for the DNA-binding cleft, 1996, **319**, 619–626. doi:
261 [10.1042/bj3190619](https://doi.org/10.1042/bj3190619)

262 23 J. T. Rhule, C. L. Hill, D. A. Judd, R. F. Schinazi, *Chem. Rev.*, Polyoxometalates in
263 Medicine, 1998, **98**, 327–358. doi: [10.1021/cr960396q](https://doi.org/10.1021/cr960396q)

264 24 B. Hasenknopf, *Frontiers Biosci.*, Polyoxometalates: introduction to a class of inorganic
265 compounds and their biomedical applications, 2005, **10**, 275–287. doi: [10.2741/1527](https://doi.org/10.2741/1527)

266 25 S. G. Mauracher, C. Molitor, R. Al-Oweini, U. Kortz, A. Rompel, *Acta Crystallogr., Sect.*
267 *D*, Latent and active abPPO4 mushroom tyrosinase cocrystallized with
268 hexatungstotellurate(VI) in a single crystal, 2014, **70**, 2301–2315. doi:
269 [10.1107/S1399004714013777](https://doi.org/10.1107/S1399004714013777)

270 26 H. Giang, T. Ly, G. Absillis, R. Janssens, P. Proost, T. N. Parac-Vogt, *Angew. Chem. Int.*
271 *Ed.*, Highly Amino Acid Selective Hydrolysis of Myoglobin at Aspartate Residues as Promoted
272 by Zirconium(IV)-Substituted Polyoxometalates, 2015, **54**, 7391–7394. doi:
273 [10.1002/anie.201502006](https://doi.org/10.1002/anie.201502006)

274 27 P. Yang, Z. Lin, B. S. Bassil, G. Alfaro-Espinoza, M. S. Ullrich, M.-X. Li, C. Silvestru, U.
275 Kortz, *Inorg. Chem*, Tetra-Antimony(III)-Bridged 18-Tungsto-2-Arsenates(V), [(LSb(III))₄(A- α -
276 As(V)W₉O₃₄)₂](10-) (L = Ph, OH): Turning Bioactivity On and Off by Ligand Substitution, 2016,
277 **55**, 3718–3720. doi: [10.1021/acs.inorgchem.6b00107](https://doi.org/10.1021/acs.inorgchem.6b00107)

278 28 M. Selman, C. Rousso, A. Bergeron, H.H. Son, R. Krishnan, N.A. El-Sayes, O. Varette, A.
279 Chen, F. Le Boeuf, F. Tzelepis, J.C. Bell, D.C. Crans, J.S. Diallo, *Mol Ther*, Multi-modal
280 Potentiation of Oncolytic Virotherapy by Vanadium compounds, 2018, **26**(1), 56-69. doi:
281 [10.1016/j.ymthe.2017.10.014](https://doi.org/10.1016/j.ymthe.2017.10.014)

282 29 K. Schmidt, G. Schrobilgen, J. Sawyer, *Acta Crystallogr. Sect. C: Cryst. Struct. Commun.*,
283 Hexasodium hexatungstotellurate(VI) 22-hydrate, 1986, **42**, 1115–1118. doi:
284 [10.1107/S0108270186093204](https://doi.org/10.1107/S0108270186093204)

285 30 Y. Chen, J. Liu, *Synth. React. Inorg. Met. Org. Chem.*, 1997, **27**, 234.

286 31 P. J. Domaille, W. H. Knoth, *Inorg. Chem.*, Ti2W10PO407- and
287 [CpFe(CO)2Sn]2W10PO385-. Preparation, properties, and structure determination by
288 tungsten-183 NMR, 1983, **22**, 818-822. doi: 10.1021/ic00147a023

289 32 M. B. Čolović, B. Medić, M. Četković, T. K. Stevović, M. Stojanović, W. W. Ayass, A. S.
290 Mougharbel, M. Radenković, M. Prostran, U. Kortz, *Toxicol. Appl. Pharmacol.*, Toxicity
291 evaluation of two polyoxotungstates with anti-acetylcholinesterase activity, 2017, **333**, 68-75.
292 doi: 10.1016/j.taap.2017.08.010

293 33 Z. Ilyas, H. S. Shah, R. Al-Oweini, U. Kortz, J. Iqbal, *Metallomics*, Antidiabetic potential
294 of polyoxotungstates: in vitro and in vivo studies, 2014, **6**, 1521–1526. doi:
295 10.1039/c4mt00106k

296 34 J. Iqbal, M. Barsukova-Stuckart, M. Ibrahim, S. U. Ali, A. A. Khan, U. Kortz, *Med. Chem.*
297 *Res.*, Polyoxometalates as potent inhibitors for acetyl and butyrylcholinesterases and as
298 potential drugs for the treatment of Alzheimer's disease, 2013, **22**, 1224–1228. doi:
299 10.1007/s00044-012-0125-8

300 35 D.L. Barnard, C.L. Hill, T. Gage, J.E. Matheson, J.H. Huffman, R.W. Sidwell, M. I Otto, R.
301 F. Schinazi, *Antiviral Res*, Potent inhibition of respiratory syncytial virus by polyoxometalates
302 of several structural classes, 1997, **34**, 27–37. [https://doi.org/10.1016/S0166-3542\(96\)01019-](https://doi.org/10.1016/S0166-3542(96)01019-4)
303 4

304 36 S. Shigeta, S. Mori, T. Yamase, N. Yamamoto, N. Yamamoto, *Biomed Pharmacother*
305 *Biomedecine Pharmacother*, Anti-RNA virus activity of polyoxometalates, 2006, **60**, 211–9.
306 doi:10.1016/j.biopha.2006.03.009

307 37 Y. Qi, Y. Xiang, J. Wang, Y. Qi, J. Li, J. Niu, J. Zhong, *Antiviral Res*, Inhibition of hepatitis C
308 virus infection by polyoxometalates, 2013, **100**, 392–8. doi: 10.1016/j.antiviral.2013.08.025

309 38 S. Shigeta, S. Mori, E. Kodama, J. Kodama, K. Takahashi, T. Yamase, *Antiviral Res*, Broad
310 spectrum anti-RNA virus activities of titanium and vanadium substituted polyoxotungstates,
311 2003, **58**, 265–71. [https://doi.org/10.1016/S0166-3542\(03\)00009-3](https://doi.org/10.1016/S0166-3542(03)00009-3)

312 39 J. Wang, Y. Liu, K. Xu, Y. Qi, J. Zhong, K. Zhang, J. Li, E. Wang, Z. Wu, Z. Kang, *ACS Appl*
313 *Mater Interfaces*, Broad-spectrum antiviral property of polyoxometalate localized on a cell
314 surface, 2014, **6**, 9785–9. doi: 10.1021/am502193f

316 **Tables**

POM sample	pH	Osmolarity (mOsm)	Zeta potential (mV)
TeW ₆	5.65	324	- 6.06 ± 3.11
TiW ₁₁ Co	5.45	320	- 6.95 ± 3.49
Ti ₂ PW ₁₀	6.25	316	- 5.31 ± 1.95

317 **Table1. Characteristics of POM aqueous solutions**

318

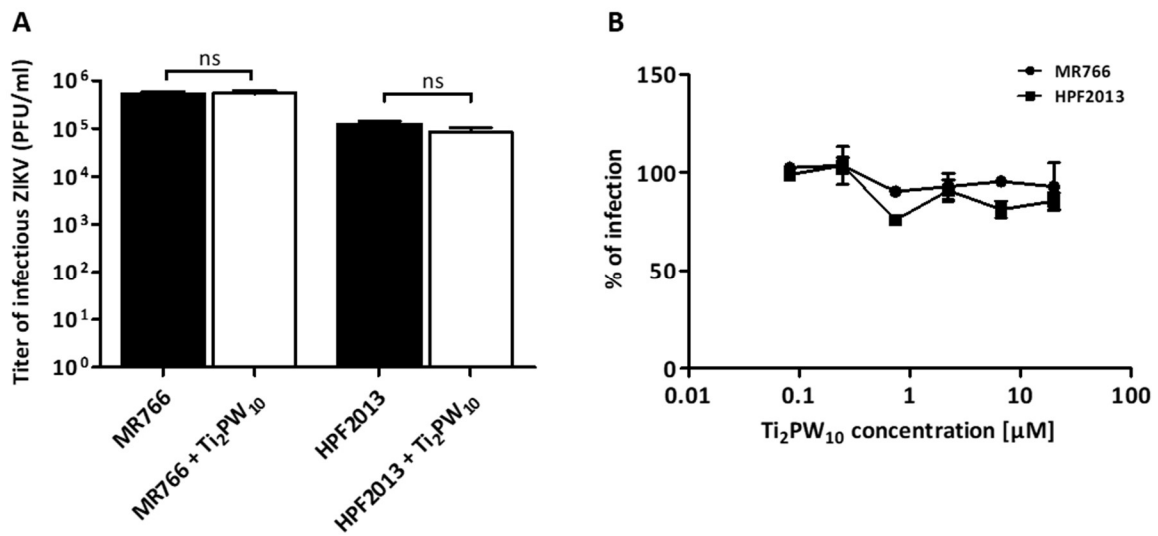
Compound	Virus	EC ₅₀ (μM) (95% CI)	EC ₉₀ (μM) (95% CI)	CC ₅₀ (μM) (95% CI)	SI
TeW ₆	MR766	2.52 (1.87 - 3.39)	9.47 (4.41 - 20.35)	210.1 (161.3 - 273.6)	83.37
	HPF2013	0.71 (0.53 - 0.96)	6.12 (3.29 -11.39)	210.1 (161.3 - 273.6)	295.91
	HRoV	n.a.	n.a.	> 75	-
TiW ₁₁ Co	MR766	1.04 (0.80 - 1.35)	5.19 (2.87 - 9.38)	97.08 (51.36 - 183.5)	93.34
	HPF2013	0.70 (0.57 - 0.87)	1.41 (1.02 - 1.94)	97.08 (51.36 - 183.5)	138.68
	HRoV	n.a.	n.a.	> 75	-
Ti ₂ PW ₁₀	MR766	0.63 (0.51 - 0.78)	3.51 (2.19 - 5.63)	> 225	> 357.14
	HPF2013	0.70 (0.59 - 0.84)	2.78 (1.82 - 4.25)	> 225	> 321.42
	HRoV	n.a.	n.a.	> 75	-

319 **Table 2. Antiviral activity of TeW₆, TiW₁₁Co and Ti₂PW₁₀**

320 EC₅₀: half maximal effective concentration; EC₉₀: 90 % effective concentration; CC₅₀: half maximal
 321 cytotoxic concentration; SI: selectivity index; n.a.: not assessable; CI: confidence interval

322

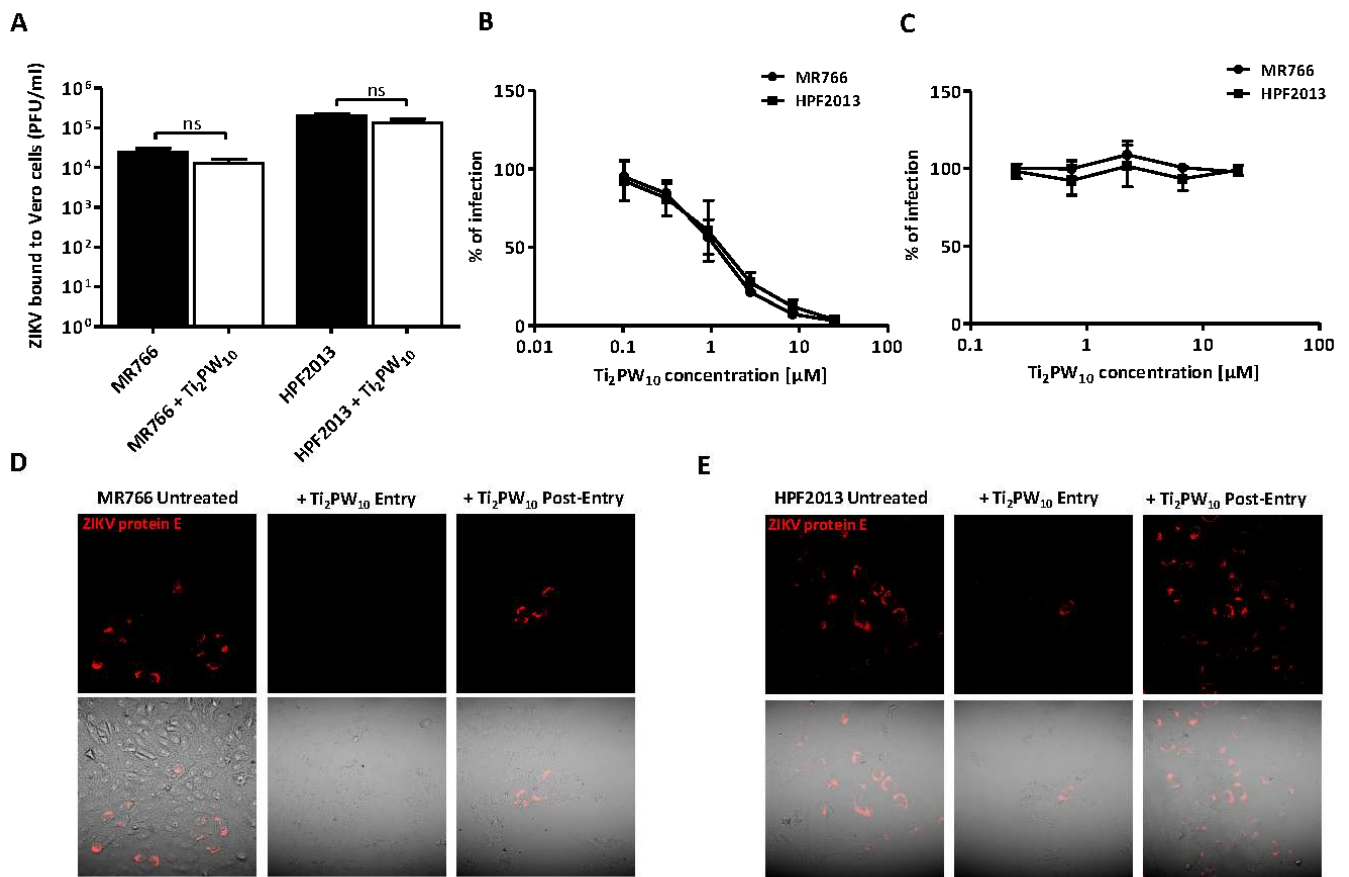
323 **Figures**



324

325 **Figure 1: Ti₂PW₁₀ does not impair extracellular viral particles and the cells pre-treatment does**
326 **not affect ZIKV infection.** Panel **A** shows the evaluation of the virucidal effect of Ti₂PW₁₀ on
327 infectious ZIKV particles. Approximately 10⁵ PFU of ZIKV (MR766 or HPF2013) plus EC₉₀ of Ti₂PW₁₀
328 were added to MEM and mixed in a total volume of 100 μL. The mixture was incubated for 2 h at
329 37°C then diluted serially to the non-inhibitory concentration of the test polyanion; the residual
330 viral infectivity was determined by viral plaque assay. Panel **B** displays the effect of cells pre-
331 treatment with Ti₂PW₁₀. Vero cells were pre-treated with serial dilutions of Ti₂PW₁₀ for 2 hours
332 before infection. After washing, cells were infected with ZIKV and the number of viral plaques was
333 evaluated after 72 hours. In panels A, the viral titers are expressed as PFU/ml and are shown as
334 mean plus SEM for three independent experiments. In panels B, the number of viral plaques in the
335 treated samples is expressed as a percentage of the untreated control and each point represents
336 mean and SEM for three independent experiments. Experimental details are described in the
337 Supplementary data file.

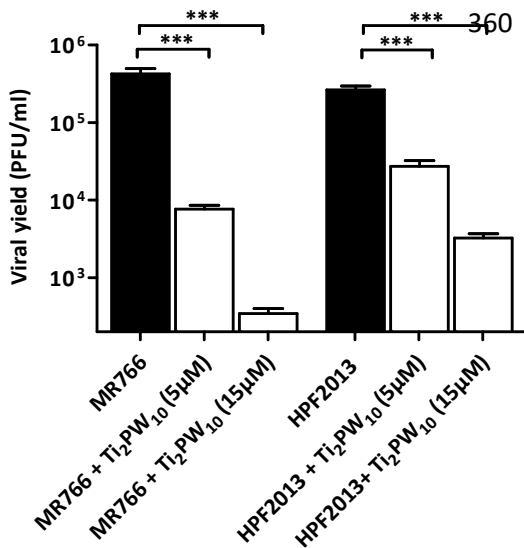
338



339 **Figure 2: Ti₂PW₁₀ hampers the entry process of ZIKV into the host cell.** In the binding assay (2A),
 340 ZIKV particles (MR766 or HPF2013, MOI=3) were allowed to attach to cells in presence of Ti₂PW₁₀
 341 (EC₉₀) for 2 h on ice. Cells were then washed to remove the unbound virus and subsequently
 342 subjected to three rounds of freeze-thawing to release bound virus. The lysate was clarified and
 343 the cell-bound virus titer was determined by viral plaque assay. Here, the viral titers are expressed
 344 as PFU/ml and are shown as mean plus SEM for three independent experiments. For the entry
 345 assay (2B), ZIKV (MR766 or HPF2013) was adsorbed for 2 h at 4°C on pre-chilled Vero cells. After
 346 the removal of the unbound virus, the temperature was shifted to 37°C to allow the entry of pre-
 347 bound virus in presence of serial dilutions of Ti₂PW₁₀. Subsequently, unpenetrated virus was
 348 inactivated with an incubation with citrate buffer followed by 3 washes. The number of viral
 349 plaques was evaluated after 72 h. For the post-entry assay (2C), the same protocol of the entry
 350 assay was performed, but adding the polyanion after the incubation with citrate buffer for 24h.
 351 The number of infected cells was assessed by indirect immunostaining after 24 h, in order to avoid
 352 the inhibition of the entry step of the upcoming viral progeny. In panels B, C, the number of viral
 353 plaques or infected cells in the treated samples is expressed as a percentage of the untreated
 354 control and each point represents mean and SEM for three independent experiments. In figures
 355 2D (MR766) and 2E (HPF2013), the entry and the post-entry assays were performed with a

356 concentration of Ti_2PW_{10} corresponding to EC_{99} . After 30 hours of infection, cells were fixed and
357 subjected to immunofluorescence. The ZIKV protein E is visualized in red. All experimental details
358 are described in the Supplementary data file.

359



361 **Figure 3: Ti_2PW_{10} reduces ZIKV progeny production.** To test the ability of Ti_2PW_{10} compound to
362 inhibit multiple cycles of ZIKV replication, Vero cells were treated and infected with a mixture of
363 Ti_2PW_{10} (5µM or 15µM) and ZIKV (MR766 or HPF2013, MOI=0.001) for 2 hours at 37°C. The virus
364 inoculum was then removed and cells were incubated with medium containing the compound
365 (5µM or 15 µM) until control cultures displayed extensive cytopathology. Supernatants were
366 clarified and cell-free virus infectivity titers were determined by the plaque assay. The viral titers
367 are expressed PFU/ml and are shown as mean plus SEM for three independent experiments.
368 (***) $P_{Tstud} < 0.001$

369

370 **Supplementary data file**

371

372 **Anti-zika virus activity of polyoxometalates**

373

374 Rachele Francese,^a Andrea Civra,^a Massimo Rittà,^a Manuela Donalisio,^a Monica Argenziano,^b
375 Roberta Cavalli,^b Ali S. Mougharbel,^c Ulrich Kortz,^{c*} and David Lembo^{a*}

376

377 ^a *Dept. of Clinical and Biological Sciences; Laboratory of Molecular Virology and Antiviral Research;*
378 *University of Turin; S. Luigi Gonzaga Hospital; Orbassano (Turin), Italy*

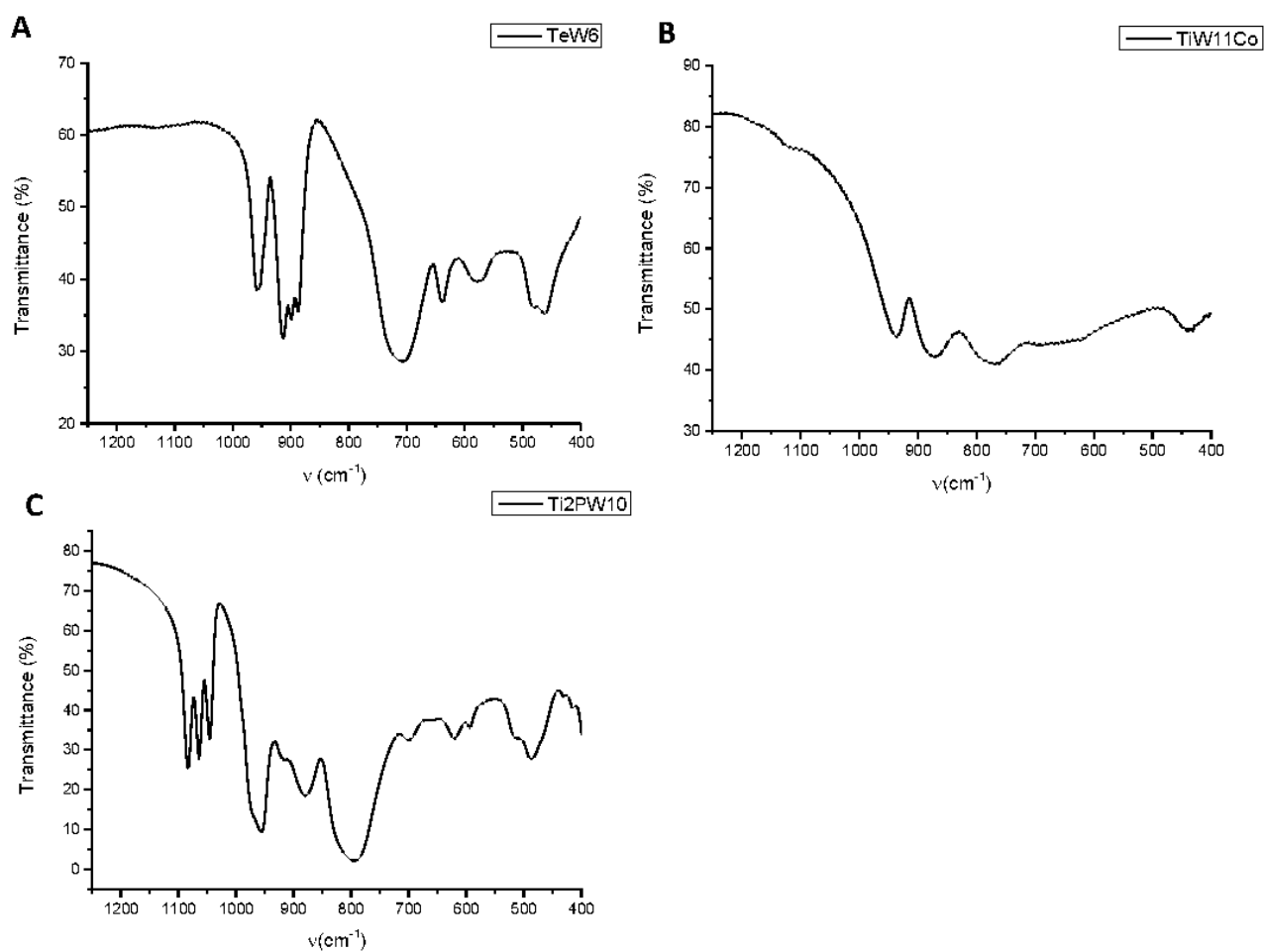
379 ^b *Dept. of Drug Science and Technology; Innovative Pharmaceutical and Cosmetic Technology and*
380 *Nanotechnology Group; University of Turin, Italy*

381 ^c *Department of Life Sciences and Chemistry, Jacobs University, Campus Ring 1, 28759 Bremen,*
382 *Germany*

383

384 **Supplementary figures:**

385



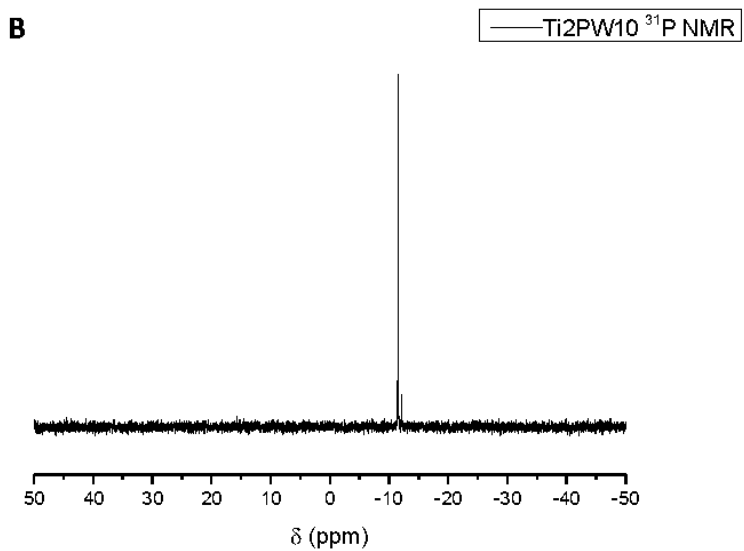
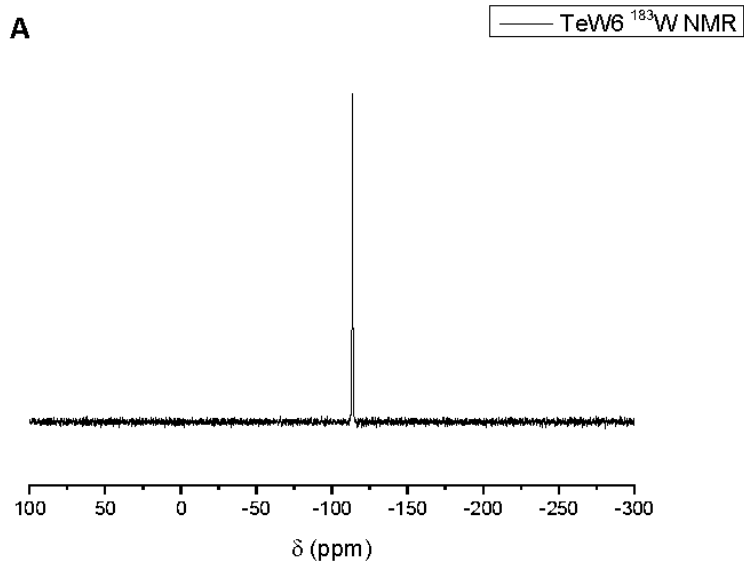
386

387

388 **Supplementary figure 1: IR characterization of TeW₆, TiW₁₁Co and Ti₂PW₁₀**

389 Panels A, B, C show the infrared spectra (finger print region) of TeW₆, TiW₁₁Co and Ti₂PW₁₀.

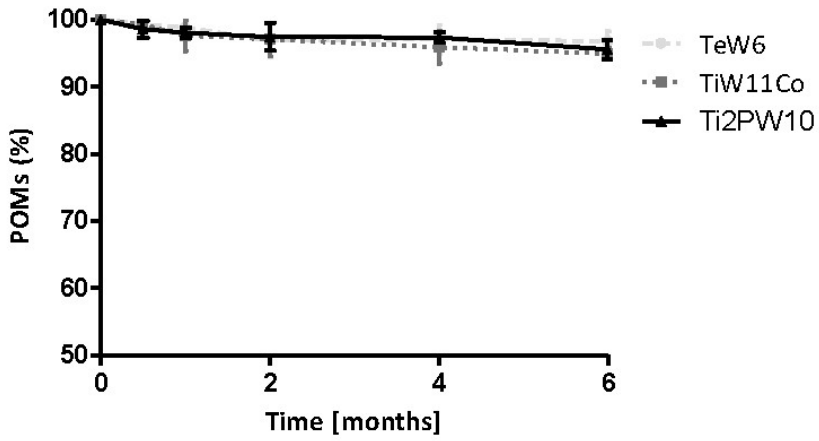
390



391

392 **Supplementary figure 2: NMR spectra of TeW₆ (¹⁸³W) (A) and Ti₂PW₁₀ (³¹P) (B) in H₂O/D₂O at room**
393 **temperature**

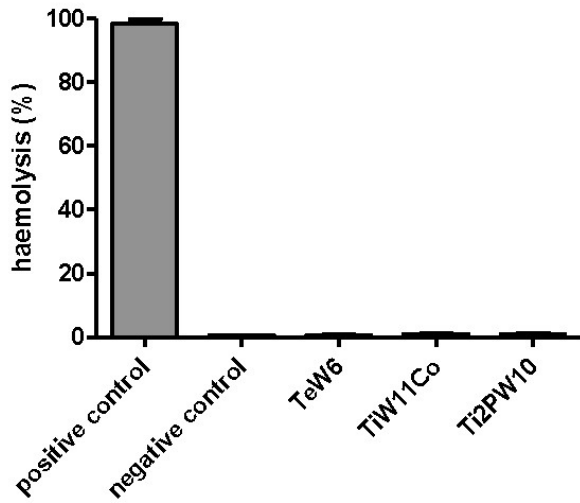
394



395

396 **Supplementary figure 3: Stability over time for TeW₆, TiW₁₁Co and Ti₂PW₁₀ polyoxometalate**
 397 **solutions**

398



399

400 **Supplementary figure 4: Hemolytic activity of aqueous POM solutions**

401

402 **Materials and methods**

403 **1. Cell lines and viruses**

404 African green monkey fibroblastoid kidney cells (Vero) (ATCC CCL-81) were cultured in Eagle's
405 minimal essential medium (MEM; Sigma, St. Louis, MO) supplemented with heat-inactivated, 10%
406 (v/v) fetal bovine serum (FBS) (Sigma). The embryonic human kidney cells (293T) (ATCC CRL-3216)
407 and the african green monkey kidney epithelial cells (MA104) (ATCC CRL-2378.1) were grown as
408 monolayer in Dulbecco's modified Eagle's medium (DMEM; Sigma) supplemented with heat-
409 inactivated 10% FBS and 1% Glutamax-I (Invitrogen, Carlsbad, CA). All media were supplemented
410 with 1% (v/v) antibiotic-antimycotic solution (Zell Shield, Minerva Biolabs, Berlin, Germany) and
411 cells were grown at 37 °C in an atmosphere of 5% of CO₂.

412 The antiviral assays against ZIKV were performed on Vero cells using MEM supplemented with 2%
413 of FBS, unless otherwise stated.

414

415 **2. Viruses production**

416 Two strains of infectious Zika viruses (1947 Uganda MR766 and 2013 French Polynesia HPF13)
417 were generated by transfection of 293T cells with two plasmids (pCDNA6.2 Zika MR766
418 Intron3115 HDVr MEG 070916 5 and pCDNA6.2 Zika HPF2013 3864,9388Intron HDVr MEG091316
419 2) kindly provided by Prof. F. Di Cunto and Prof. M. J. Evans.^{1,2} Briefly, one day prior to
420 transfection, 2.3x10⁶ 293T cells were seeded in 100mm tissue culture dishes. 4.5 µg of plasmid
421 DNA were incubated with 27µl of Lipofectamine (Thermo Fisher Scientific, California, USA) and
422 Opti-MEM (Sigma) in a final volume of 900µl for 5 minutes at room temperature. The mixture was
423 then used to transfect cells in a final volume of 5.5 ml of DMEM 10% FBS without antibiotics, for 5
424 hours at 37°C in 5% of CO₂ atmosphere. Supernatants from transfected cells were collected 5 or 15
425 days post transfection (MR766 and HPF2013 strain respectively) and then titrated by plaque assay.

426 HRoV Wa (ATCC® VR-2018) were purchased from ATCC and activated with 5 µg/ml of porcine
427 pancreatic trypsin type IX (Sigma, St. Louis, Mo.) for 30 min at 37 °C. It was propagated in MA104
428 cells by using DMEM containing 0.5 µg of trypsin per ml as previously described.³

429

430 **3. Synthesis of POMs**

431 **3.1 Synthesis of Na₆[TeW₆O₂₄]·22H₂O:**

432 A solution was prepared by dissolving 5.0 g (15.2 mmol) of Na₂WO₄·2H₂O and 0.6 g (2.6
433 mmol) of Te(OH)₆ in 100 mL of water. The pH was adjusted to 5.0 using HCl (1 M) followed
434 by heating at 100 °C until the volume of the solution was about 75 ml. The solution was
435 allowed to cool to room temperature and filtered. The filtrate was left at room
436 temperature in an open beaker for one week and led to the formation of colorless crystals,
437 which were collected by filtration and air-dried.

438

439 **3.2 Synthesis of K₇[Ti₂W₁₀PO₄₀]·6H₂O:**

440 6.0 g (43 mmol) of NaH_2PO_4 were added to a stirred solution of $\text{Na}_2\text{WO}_4 \cdot 2\text{H}_2\text{O}$ (30.0 g, 91
441 mmol) in water (100 ml) followed by dropwise addition of 1.8 ml (16 mmol) of TiCl_4 . The
442 obtained white suspension was refluxed for 2 hours, cooled to room temperature and
443 filtered. The filtrate was treated with 30 g of solid KCl and the white precipitate was
444 collected by filtration. The precipitate was recrystallized in hot water to obtain the pure
445 compound.

446

447 **3.3 Synthesis of $\text{K}_6\text{H}[\text{TiCoW}_{11}\text{O}_{40}]$:**

448 18.2 g (55 mmol) of $\text{Na}_2\text{WO}_4 \cdot 2\text{H}_2\text{O}$ were dissolved in 100 ml of water and the pH of the
449 solution was adjusted to 6.3 using glacial acetic acid. To this solution, 10 ml of 0.52 M
450 cobalt acetate solution were added. The obtained red solution was heated to 80 °C for
451 approximately one hour until the color turned blue. To this solution, 10 ml of 1 M TiOSO_4
452 solution in 0.1 M H_2SO_4 were added dropwise under vigorous stirring. The pale blue
453 mixture was refluxed for one hour, cooled to room temperature and treated with 10 g KCl.
454 The precipitate was then filtered and the filtrate was cooled to 0 °C. Finally, 200 ml of
455 ethanol were added to the filtrate and the light blue precipitate was collected by suction
456 filtration.

457

458 **4. Preparation of TeW_6 , TiW_{11}Co and $\text{Ti}_2\text{PW}_{10}$ solutions**

459 The three POM salts $\text{Na}_6[\text{TeW}_6\text{O}_{24}] \cdot 22\text{H}_2\text{O}$ (Na- TeW_6), $\text{K}_6\text{H}_2[\text{TiW}_{11}\text{CoO}_{40}] \cdot 13\text{H}_2\text{O}$ (K- TiW_{11}Co), and
460 $\text{K}_7[\text{Ti}_2\text{PW}_{10}\text{O}_{40}] \cdot 6\text{H}_2\text{O}$ (K- $\text{Ti}_2\text{PW}_{10}$) were dissolved under mild stirring at room temperature in saline
461 solution (NaCl 0.9% w/v) at the concentration of 2 mg/ml.

462

463 **5. Characterization of TeW_6 , TiW_{11}Co and $\text{Ti}_2\text{PW}_{10}$ solutions**

464 The pH of the POM aqueous solutions was recorded at room temperature using a pH meter Orion
465 model 420A.

466 The osmolarity of the POM aqueous solutions was measured using a Semi-Micro Osmometer K-
467 7400 Knauer, at room temperature.

468 The zeta potential was determined by electrophoretic mobility using a 90 Plus instrument
469 (Brookhaven, NY, USA). The analysis was performed at room temperature, using POM aqueous
470 solutions diluted with NaCl 0.9% w/v (1:10 v/v). For the zeta potential evaluation, samples of
471 diluted formulations were placed in the electrophoretic cell, where an electric field of
472 approximately 15 V/cm was applied.

473

474 **6. Quantitative determination of POMs**

475 The quantitative determination of the POMs in the aqueous solutions was performed using UV-VIS
476 spectrophotometer (Beckman Coulter DU730). A preliminary evaluation of the UV spectra of the

477 compounds was carried out by spectrophotometric analysis collecting the absorbance data in the
478 range between 200 and 800 nm to identify the absorbance maximum (λ_{max}) peak.

479 Linear calibration curves were obtained over the concentration range of 0–100 $\mu\text{g}/\text{mL}$, with a
480 regression coefficient of 0.999 for all the compounds.

481

482 **7. Stability overtime of TeW_6 , TiW_{11}Co and $\text{Ti}_2\text{PW}_{10}$ solutions**

483 The stability of polyoxometalate aqueous solutions was evaluated over time, determining the
484 POM concentrations in the solutions by UV-VIS spectroscopy analysis.

485

486 **8. Evaluation of TeW_6 , TiW_{11}Co and $\text{Ti}_2\text{PW}_{10}$ solution biocompatibility**

487 To assess the biocompatibility of POM aqueous solutions the hemolysis assay was performed.

488 For hemolytic activity determination, 100 microliters of samples were incubated at 37°C for 90 min
489 with 1 ml of diluted blood (1:4 v/v) obtained by adding freshly prepared PBS at $\text{pH} = 7.4$. After
490 incubation, sample-containing blood was centrifuged at 1000 rpm for 5 minutes to separate
491 plasma. The amount of hemoglobin released due to hemolysis was determined
492 spectrophotometrically (absorbance readout at 543 nm using a Duo spectrophotometer,
493 Beckman). The hemolytic activity was calculated to reference with a negative control consisting of
494 diluted blood without the addition of the samples. Complete hemolysis was induced by the
495 addition of ammonium sulfate (20 % w/v). Optical microscopy was used to evaluate changes on
496 red blood cell morphology after incubation with the formulations.

497

498

499

500 **9. ZIKV titration by plaque assay**

501 Vero cells, seeded the day before at a density of 6×10^3 in 96 well plates, were inoculated with
502 increasing dilutions of virus prepared in cold MEM with 2% of FBS. After 2h adsorption at 37°C , the
503 virus inoculum was removed, cells overlaid with 1.2% methylcellulose and incubated at 37°C for
504 72h. Plates were then fixed and colored with 0.1% of crystal violet for 30 minutes and then gently
505 washed with water. The virus titer was estimated as plaque forming units per ml (PFU/ml) by
506 counting the number of plaques at an appropriate dilution.

507

508 **10. Viability Assay**

509 Cell viability was measured using the MTS [3-(4,5-dimethylthiazol-2-yl)-5-(3-
510 carboxymethoxyphenyl)-2-(4-sulfophenyl)-2H-tetra-zolium] assay. Vero cells were seeded at a
511 density of $6 \times 10^3/\text{well}$ in 96-well plates and treated, the following day, with different concentration

512 of **TeW₆**, **TiW₁₁Co** and **Ti₂PW₁₀** compounds under the same experimental conditions described for
513 the ZIKV inhibition assays. Cell viability was determined using the Cell Titer 96 Proliferation Assay
514 Kit (Promega, Madison, WI, USA) according to the manufacturer's instructions. Absorbances were
515 measured using a Microplate Reader (Model680, BIORAD) at 490 nm. The effect on cell viability at
516 different concentrations of the compound was expressed as a percentage, by comparing
517 absorbances of treated cells with those of cells incubated with culture medium alone. The 50%
518 cytotoxic concentrations (CC₅₀) was determined using Prism software (Graph-PadSoftware, San
519 Diego, CA).

520

521 **11. ZIKV inhibition assays**

522 The effect of **TeW₆**, **TiW₁₁Co** and **Ti₂PW₁₀** on ZIKV infection was evaluated by plaque reduction
523 assay. Vero cells were pre-plated 24h in advance in 24-well plates at a density of 7x10⁴ cells. The
524 **TeW₆**, **TiW₁₁Co** and **Ti₂PW₁₀** were serially diluted in medium (from 25μM to 0.0016 μM) and added
525 to cell monolayers. After 2h of incubation at 37°C, medium was removed and infection was
526 performed with 250 μL/well of MR766 or HPF2013 (MOI = 0.0005) and different concentrations of
527 the POMs, for 2h at 37°C. The virus inoculum was then removed and the cells washed and overlaid
528 with a medium containing 1.2% methylcellulose (Sigma) and serial dilutions of the POMs. After an
529 incubation at 37°C for 72h, cells were fixed and stained with 0.1% crystal violet in 20% ethanol and
530 viral plaques counted. The effective concentration producing 50% reduction in plaque formation
531 (EC₅₀) was determined using Prism software by comparing treated with untreated wells. The
532 selectivity index (SI) was calculated by dividing the CC₅₀ by the EC₅₀ value.

533

534 **12. Rotavirus inhibition assay**

535 To assess the ability of **TeW₆**, **TiW₁₁Co** and **Ti₂PW₁₀** to inhibit rotavirus infectivity, inhibition assays
536 were carried out with MA104 cells seeded at a density of 1,4x10⁴ cells/well in 96-well plates.
537 Similarly to the ZIKV inhibition assay, cells were pre-treated with serial dilutions of **TeW₆**, **TiW₁₁Co**
538 and **Ti₂PW₁₀** (from 25μM to 0.0016 μM) for 2h at 37°C. Then, the medium was removed and the
539 infection was performed with trypsin-activated rotavirus (MOI = 0.02) and different
540 concentrations of the polyoxometalates for 1h. After incubation, cells were washed with medium
541 and incubated with serial dilutions of POMs for 16h. Next, cells were fixed with cold acetone-
542 methanol (50:50), and the number of infected cells were determined by indirect immunostaining
543 by using a mouse monoclonal antibody directed to human rotavirus VP6 (0036; Villeurbanne,
544 France), and the secondary antibody peroxidase-conjugated AffiniPure F(ab')₂ Fragment Goat
545 Anti-Mouse IgG (H + L) (Jackson ImmunoResearch Laboratories Inc., 872 W. Baltimore Pike, West
546 Grove, PA 19390).

547

548

549

550 **13. ZIKV yield reduction assay**

551 To test the ability of **Ti₂PW₁₀** compound to inhibit multiple cycles of ZIKV replication, Vero cells
552 were seeded at a density of 5×10^4 cells/well in 24 well-plates. The day after, cells were treated and
553 infected in duplicate with a mixture of **Ti₂PW₁₀** (5 μ M or 15 μ M) and ZIKV (MR766 or HPF2013,
554 MOI=0.001) for 2 hours at 37°C. Following virus adsorption, the virus inoculum was removed and
555 cells were incubated with medium containing the compound (5 μ M or 15 μ M) until control cultures
556 displayed extensive cytopathology. Supernatants were clarified and cell-free virus infectivity titers
557 were determined in duplicate by the plaque assay on Vero cell monolayers.

558
559 **14. Ti₂PW₁₀ mechanism of action against ZIKV**

560 **14.1 Virus inactivation assay**

561 Approximately 10^5 PFU of MR766 or HPF2013 plus EC₉₀ of **Ti₂PW₁₀** were added to MEM and mixed
562 in a total volume of 100 μ l. The virus-compound mixture was incubated for 2h at 37°C then diluted
563 serially to the non-inhibitory concentration of test compound; the residual viral infectivity was
564 determined by viral plaque assay.

565
566 **14.2 Cell pre-treatment assay**

567 To evaluate the antiviral activity of compound when administered before infection, confluent Vero
568 cells in 24 well plates (7×10^4 cells/well) were pre-treated with different concentrations of **Ti₂PW₁₀**
569 (from 20 μ M to 0.08 μ M) for 2 hours at 37°C. After washing, cells were infected with MR766 or
570 HPF2013 at MOI=0.0005 for two hours, then washed and overlaid with 1.2% methylcellulose
571 medium for 72h at 37°C. At the end of the incubation cells were fixed and stained with 0.1%
572 crystal violet in 20% ethanol to count the number of viral plaques.

573
574 **14.3 Binding assay**

575 Vero cells were seeded in 24-well plates at a density of 1.1×10^5 . The following day, cells and virus
576 (MR766 or HPF2013 virus, MOI=3) were cooled to 4°C for 10 minutes and then the virus was
577 allowed to attach to cells on ice in presence of the **Ti₂PW₁₀** compound (EC₉₀). After an incubation
578 of 2h on ice, cells were washed with cold MEM, followed by addition of fresh cold medium. Cells
579 were subjected to three rounds of freeze-thawing to release bound virus and the lysate clarified
580 by low speed centrifugation for 10 minutes. Cell-bound virus titers were determined by viral
581 plaque assay.

582
583 **14.4 Entry assay**

584 For entry assays, MR766 and HPF2013 (MOI=0.005) were adsorbed for 2h at 4°C on pre-chilled
585 confluent Vero cells in 24-well plates. Cells were then washed twice with cold MEM to remove the
586 unbound virus and then incubated with serial dilutions of **Ti₂PW₁₀** compound for 2h at a
587 temperature of 37°C to allow virus entry. Unpenetrated viruses were inactivated with citrate

588 buffer (citric acid 40 mM, potassium chloride 10 mM, sodium chloride 135 mM, pH 3) for 1min at
589 room temperature, as previously described.^{4,5} Cells were then washed with warm medium 3 times
590 and overlaid with 1.2% methycellulose medium. After 3 days of incubation, cells were fixed and
591 stained with 0.1% crystal violet in 20% ethanol to count the number of viral plaques.

592

593 **14.5 Post entry assay: focus reduction assay**

594 To evaluate the antiviral activity of **Ti₂PW₁₀** compound when administered after infection, Vero
595 cells were seeded in 96 well-plates at a density of 1,3x10⁴ cells/well. The following day, ZIKV
596 (MR766 or HPF2013, MOI=0.01) was allowed to attach to pre-cooled cells for 2 hours at 4°C. Then,
597 two gentle washes were performed and cells were incubated at 37°C for 2 hours to allow virus
598 penetration into the host cell. Unpenetrated viruses were inactivated with citrate buffer for 1min
599 at room temperature and cells were subsequently washed with warm medium 3 times and
600 incubated with serial dilutions of **Ti₂PW₁₀** (from 20µM to 0.08µM). After 24 hours cells were fixed
601 with acetone-methanol (50:50). The number of infected cells were determined by indirect
602 immunostaining by using a mouse monoclonal antibody direct to flavivirus protein E (D1-4G2-4-15
603 (4G2), Novus Biological) and a secondary antibody peroxidase-conjugated AffiniPure F(ab')₂
604 Fragment Goat Anti-Mouse IgG (H+L) (Jackson ImmunoResearch Laboratories Inc., 872 W.
605 Baltimore Pike, West Grove, PA 19390). Immunostained cells were counted, and the percent
606 inhibition of virus infectivity determined by comparing the number of infected cells in treated
607 wells with the number in untreated control wells.

608

609 **14.6 Immunofluorescence experiments**

610 Subconfluent Vero cell monolayers plated on coverslips in 24-well plates were treated with
611 **Ti₂PW₁₀** (EC₉₉) during the entry of ZIKV into cells or during the post-entry phase. First, the
612 virus (MR766 or HPF2013, MOI=5) was allowed to attach to pre-chilled cells for 2 hours on
613 ice. Subsequently, after the removal of the unbound virus with a gentle wash, the
614 temperature was shifted to 37°C in order to allow the virus entry. For the entry assay, the
615 polyanion was added at this time point. After 2 hours of virus adsorption, the
616 unpenetrated virus was inactivated with citrate buffer (as previously described) for 1min at
617 room temperature. Three gentle washes were readily performed and fresh medium was
618 added to cells for 30 h. For the post-entry assay, the polyanion was added to cells at this
619 time point (for 30 h). Subsequently, cells were washed twice with PBS and fixed in
620 paraformaldehyde 4% for 15 min at room temperature. After three washes with PBS, cells
621 were permeabilized with PBS-Triton 0.1% for 20 min on ice. Cells were then blocked with
622 5% BSA for 15 min and then incubated with the primary antibody (a mouse monoclonal
623 antibody direct to flavivirus protein E (D1-4G2-4-15 (4G2), Novus Biological) diluted in
624 blocking buffer + 0.05% Tween 20 for 1h at room temperature. Three washes in PBS with
625 0.05% Tween 20 were subsequently performed followed by an incubation with the
626 secondary antibody (goat anti-mouse IgG rhodamine conjugated, Santa Cruz
627 Biotechnology) diluted in blocking buffer + 0.05% Tween 20 for 1 h at room temperature.

628 After washing three times with PBS, coverslips were mounted and analysed on a confocal
629 fluorescence microscope (LSM510, Carl Zeiss, Jena, Germany).

630

631 **15. Data analysis**

632 All results are presented as the mean values from three independent experiments performed in
633 duplicate. The EC₅₀ values for inhibition curves were calculated by regression analysis using the
634 software GraphPad Prism version 5.0 (GraphPad Software, San Diego, California, U.S.A.) by fitting a
635 variable slope-sigmoidal dose-response curve.

636

637

638 **ESI references:**

- 639 1) Ghouzzi VE, Bianchi FT, Molineris I, Mounce BC, Berto GE, Rak M, et al. ZIKA virus elicits P53
640 activation and genotoxic stress in human neural progenitors similar to mutations involved in
641 severe forms of genetic microcephaly and p53. *Cell Death Dis.* 2016 Oct;7(10):e2440. doi:
642 10.1038/cddis.2016.446.
- 643 2) Schwarz MC, Sourisseau M, Espino MM, Gray ES, Chambers MT, Tortorella D, et al. Rescue of
644 the 1947 Zika Virus Prototype Strain with a Cytomegalovirus Promoter-Driven cDNA Clone.
645 *mSphere.* 2016 Oct;1(5). doi:[10.1128/mSphere.00246-16](https://doi.org/10.1128/mSphere.00246-16)
- 646 3) Coulson BS, Fowler KJ, Bishop RF, Cotton RG. Neutralizing monoclonal antibodies to human
647 rotavirus and indications of antigenic drift among strains from neonates. *J Virol.* 1985
648 Apr;54(1):14–20.
- 649 4) Talarico L, Pujol C, Zibetti R, Faria P, Nosedà M, Duarte M, et al. The antiviral activity of
650 sulfated polysaccharides against dengue virus is dependent on virus serotype and host cell.
651 *Antiviral Res.* 2005 Jun;66(2–3):103–10. doi:[10.1016/j.antiviral.2005.02.001](https://doi.org/10.1016/j.antiviral.2005.02.001)
- 652 5) Li C, Deng Y-Q, Wang S, Ma F, Aliyari R, Huang X-Y, et al. 25-Hydroxycholesterol Protects Host
653 against Zika Virus Infection and Its Associated Microcephaly in a Mouse Model. *Immunity.*
654 2017 Mar;46(3):446–56. doi:[10.1016/j.immuni.2017.02.012](https://doi.org/10.1016/j.immuni.2017.02.012)

655

656